NREL
NATIONAL RENEWABLE ENERGY LABORATORY

Optical-Fiber-Based, Time-Resolved Photoluminescence Spectrometer for Thin-Film Absorber Characterization and Analysis of TRPL Data for CdS/CdTe Interface

Preprint

Darius Kuciauskas, Joel N. Duenow, Ana Kanevce, Jian V. Li, Matthew R. Young, Pat Dippo, and Dean H. Levi

Presented at the 2012 IEEE Photovoltaic Specialists Conference
Austin, Texas
June 3–8, 2012

NREL is a national laboratory of the U.S. Department of Energy, Office of Energy Efficiency & Renewable Energy, operated by the Alliance for Sustainable Energy, LLC.

Conference Paper
NREL/CP-5200-54119
June 2012

Contract No. DE-AC36-08GO28308

NOTICE

The submitted manuscript has been offered by an employee of the Alliance for Sustainable Energy, LLC (Alliance), a contractor of the US Government under Contract No. DE-AC36-08GO28308. Accordingly, the US Government and Alliance retain a nonexclusive royalty-free license to publish or reproduce the published form of this contribution, or allow others to do so, for US Government purposes.

This report was prepared as an account of work sponsored by an agency of the United States government. Neither the United States government nor any agency thereof, nor any of their employees, makes any warranty, express or implied, or assumes any legal liability or responsibility for the accuracy, completeness, or usefulness of any information, apparatus, product, or process disclosed, or represents that its use would not infringe privately owned rights. Reference herein to any specific commercial product, process, or service by trade name, trademark, manufacturer, or otherwise does not necessarily constitute or imply its endorsement, recommendation, or favoring by the United States government or any agency thereof. The views and opinions of authors expressed herein do not necessarily state or reflect those of the United States government or any agency thereof.

Available electronically at http://www.osti.gov/bridge

Available for a processing fee to U.S. Department of Energy
and its contractors, in paper, from:

U.S. Department of Energy
Office of Scientific and Technical Information

P.O. Box 62
Oak Ridge, TN 37831-0062
phone: 865.576.8401
fax: 865.576.5728
email: mailto:reports@adonis.osti.gov

Available for sale to the public, in paper, from:

U.S. Department of Commerce
National Technical Information Service
5285 Port Royal Road
Springfield, VA 22161
phone: 800.553.6847
fax: 703.605.6900
email: orders@ntis.fedworld.gov
online ordering: http://www.ntis.gov/help/ordermethods.aspx

Cover Photos: (left to right) PIX 16416, PIX 17423, PIX 16560, PIX 17613, PIX 17436, PIX 17721

Printed on paper containing at least 50% wastepaper, including 10% post consumer waste.

Optical-Fiber-Based, Time-Resolved Photoluminescence Spectrometer for Thin-Film Absorber Characterization and Analysis of TRPL Data for CdS/CdTe Interface

Darius Kuciauskas, Joel N. Duenow, Ana Kanevce, Jian V. Li, Matthew R. Young, Pat Dippo, and Dean H. Levi

National Renewable Energy Laboratory, Golden, CO 80401-3305, USA

***Abstract* — We describe the design of a time resolved photoluminescence (TRPL) spectrometer for rapid semiconductor absorber characterization. Simplicity and flexibility is achieved by using single optical fiber to deliver laser pulses and to collect photoluminescence. We apply TRPL for characterization of CdS/CdTe absorbers after deposition, $CdCl_2$ treatment, Cu doping, and back contact formation. Data suggest this method could be applied in various stages of PV device processing. Finally, we show how to analyze TRPL data for CdS/CdTe absorbers by considering laser light absorption depth and intermixing at CdS/CdTe interface.**

***Index Terms* – Time-resolved photoluminescence, lifetime, CdTe, thin-film photovoltaics.**

I. Introduction

Development of rapid and contactless methods to evaluate thin-film PV absorber quality is highly desirable. In principle, photoluminescence (PL) spectroscopy is very useful for absorber characterization. Time-resolved PL (TRPL) spectroscopy provides additional dimension for the analysis and is especially useful for characterization of polycrystalline materials with typically broad and structure-less PL spectra. TRPL is a standard method to determine minority carrier lifetime and interface recombination velocity in III-V double heterostructures (DHs) [1]. However, DHs are not typically used in thin-film PV research. Empirically, lifetimes determined with TRPL have shown excellent correlations with open-circuit voltage, Voc, for CdS/CdTe PV devices [2] and for CdS/CIGS absorbers [3]. Thus it appears that TRPL lifetime determination offers a direct way to rapidly evaluate material processing changes that might lead to higher Voc. This is a useful result, as achieving higher Voc is generally regarded as the most promising approach to increasing thin-film PV device efficiency.

Two challenges appear to limit wider TRPL use in thin film PV research and in online diagnostics. First, TRPL instrumentation is sometimes considered to be too complex. Second, it is not simple to interpret TRPL data in terms of PV device physics. This paper describes progress addressing both of these challenges.

II. Experimental

CdS/CdTe photovoltaic solar cells were fabricated as follows. The front contact, a bilayer of 450 nm of conductive (F-doped) and 150 nm of intrinsic SnO_2, was deposited by chemical vapor deposition onto Corning 7059 glass substrates maintained at 550ºC. The CdS window layer was deposited by chemical bath deposition at 92°C to a thickness of 100 nm. The CdTe absorber layer was deposited by close-spaced sublimation (CSS) to a thickness of 4-5 µm at a substrate temperature of 620 ºC. A $CdCl_2$ vapor heat treatment was performed by CSS in an O_2/He ambient at a temperature of 400 ºC for 5 min. Next, samples were preheated for 120 min. at 300 ºC and maintained at this temperature through the pre-contact ion milling and Cu-doped ZnTe (ZnTe:Cu) back contact interface layer deposition. Ar ion-beam milling was performed to expose a stoichiometric CdTe surface (by removing ~150 nm of material) using a Kaufman-type ion source operating at a beam energy of 500 eV and a beam current of 6 mA. ZnTe:Cu films were deposited by radio-frequency (RF) magnetron sputtering to a thickness of 500 nm at a sputtering pressure of 10 mTorr Ar from ZnTe:Cu targets.

Samples were then annealed in situ for 40 min. and subsequently allowed to cool in the Ar ambient. The transparent back contact was formed by depositing indium tin oxide (using a target containing 9 wt.% SnO_2 in In_2O_3) by RF magnetron sputtering at room temperature (RT) in 10 mTorr Ar to a thickness of ~90 nm. The contact was finalized with a metal grid of 50 nm Ni and 3 µm Al deposited by electron beam evaporation at RT. While transparent back contacts are not typically used in CdS/CdTe PV devices, such contacts allow optical measurements from both sides of PV devices. Earlier papers compared properties of PV devices with different back contacts, including transparent contacts used in this study [7]. Cells of area 0.42 cm^2 were patterned by mechanical scribe. Analysis was performed at several stages of fabrication on samples that were processed identically until removed for examination.

III. Results And Discussion

A. Rapid TRPL Measurements Using Spectrometer Based on Optical Fibers

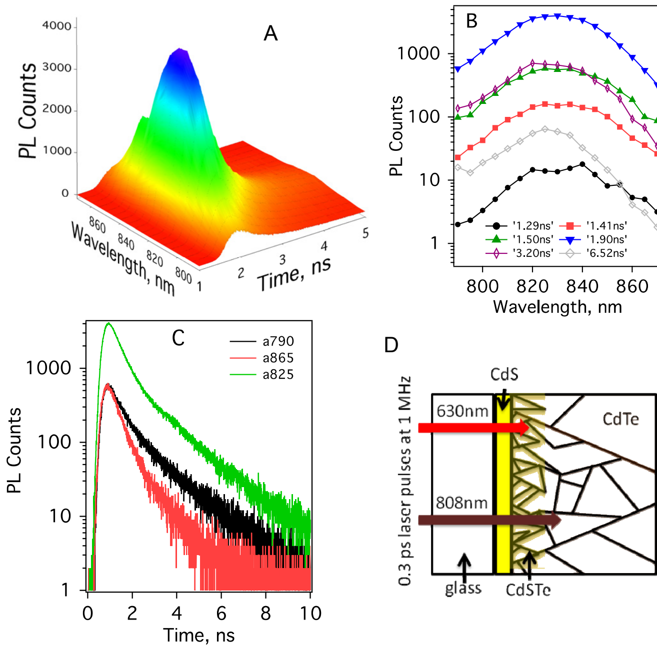

Fig. 1. A: TRPL data for CdS/CdTe PV device "2DA" at 790-870 nm and 0-5 ns. The vertical axis represents PL intensity. B: Several time-resolved PL spectra from A. Time delay at which spectra were collected is shown in the legend. C: Several TRPL decays from A (at 790 nm, 825 nm and 865 nm). D: Illustration of CdS/CdTe device and measurement configuration. Data were collected using 640 nm excitation, 2 nJ energy per 0.3 ps laser pulse (2 mW average power, repetition rate 1 MHz), and 0.17 mm laser beam diameter.

A detailed TRPL data set for CdS/CdTe PV device is shown in Fig. 1A. One axis shows temporal, the second axis spectral dependence. Amplitude represents PL signal (total counts collected per 150 s) at a specific wavelength and time delay after excitation with short (0.3 ps) laser pulse. A cross-section of this 3D data at any given time would give time-resolved PL spectra, for example at 1.29 – 6.52 ns (1B). A cross-section at, for example, 825 nm would give a PL decay that represents time-dependence of carrier recombination (1C). Thus, TRPL spectroscopy provides both spectral and time-dependent information about recombination processes.

Earlier reports considered only PL decays measured at a single wavelength, typically at PL maximum [2, 9]. Here we show that careful analysis of time-dependent spectra provides additional information about PV device performance. This characteristic is largely based on different bandgaps of CdS, CdS_xTe_{1-x} (intermixed layer at CdS and CdTe interface) and CdTe. Decays measured at different energies (different wavelengths) to some extent allow selective probing of carrier dynamics in different spatial regions of the PV device. This is evident, for example, from comparison of 790 nm (1.57 eV, CdTe emission region) and 865 nm (1.43 eV, CdS_xTe_{1-x} emission region) decays in Fig. 1C. The decay at 865nm is faster, therefore recombination and carrier dynamics in the front region (CdS_xTe_{1-x}) of the device are faster than the dynamics in the CdTe region (decay at 790 nm). Comparison of spectra measured at different time delays, for example similar amplitude spectra at 1.29 ns and 6.52 ns in 1B, also illustrates that decays at different wavelengths (energies) have different time dependence – recombination at longer wavelengths is faster than recombination at shorter wavelengths. Analysis of these data in terms of exponential decay functions is presented below.

Additional flexibility is provided by varying excitation wavelength. For example, 640 nm excitation light has absorption depth <0.3 µm, while near-bandgap excitation at 800 nm is absorbed deeper in the sample. If the measurement has sufficiently high time resolution, comparison of 640 nm vs. 800 nm excitation TRPL data allows following recombination dynamics starting from different initial carrier distribution. This will be illustrated in Fig. 6 below.

Data in Fig. 1 were collected using the experimental scheme in Fig. 2. TRPL measurement requires exciting the sample with a short laser pulse. Optical parametric amplifiers (OPA) provide a versatile source of laser pulses that are broadly tunable and have high repetition rate and sufficient energy per pulse. Because of its compact footprint, an OPA pumped by an amplified Yb : KGW (ytterbium-doped potassium gadolinium tungstate) laser was used. The time resolution of the TRPL spectrometer typically is determined by the time response of the detector; usually a PMT. R5509 PMT (Hamamatsu) allows measurements at wavelengths up to 1350 nm with ~300 ps instrument response function (IRF). A monochromator is used to select measurement wavelength. Because typical PL spectra for polycrystalline materials are broad, high spectral resolution is not required; 0.25 m monochromator with high numerical aperture is sufficient. Data shown here were collected with 2 nm spectral resolution.

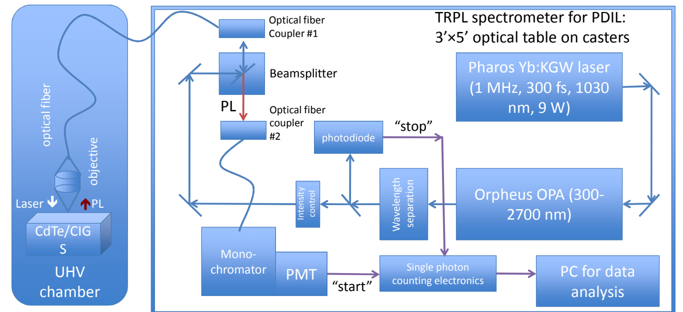

Fig. 2. Scheme of optical fiber based TRPL spectrometer. A single fiber is used to deliver laser pulses to the sample and to collect PL signals.

The difference between a conventional TRPL experimental arrangement and that shown in Fig. 2 is that optical fiber was employed to deliver optical pulses to the sample and to collect

PL signals. Optical fibers have been used in fluorescence spectroscopy and microscopy, including delivery of ultrafast pulses [4]. We find that this approach also works well for time-resolved PL measurements – and in addition provides flexibility in collecting data outside of a dedicated spectroscopy laboratory. For example, a 2-m long optical fiber was used to measure TRPL decays inside a high vacuum chamber in the Process Development and Integration Laboratory at NREL. The sample is handled by a manufacturing robot, and for TRPL analysis it is only necessary to bring measurement optics to within several millimeters of the sample surface. As measurement is contactless, no electrical connections to the sample are necessary. The same optical fiber allows for delivery of the laser pulses and for PL signal collection. Laser excitation spot size depends on optics used in setup. For data shown in this paper, the excitation spot diameter was 0.17 mm.

For convenience, a second optical fiber was used to deliver PL signal to the monochromator and the PMT detector. Time-correlated single photon counting (TCSPC) detection technique was used [5]. The principal advantage of TCSPC is that it allows deconvolution of the instrumental response from the recorded data, which improves time resolution of the measurement up to 5-10 times [5]. This is necessary for measurements in near-IR, where PMTs have relatively long IRFs. The limitation is that only one PL photon is recorded per 50-100 laser pulses, thus a laser with high repetition rate is necessary [5]. Fig. 3A shows TRPL decays recorded with a 1-MHz laser and 20-kHz photon counting rate after integration for 1-120 s. Signal amplitude increases with the longer measurement time, but 2-5 s integration provided signal/noise ratio sufficiently high for analysis as described below.

In the ideal case (e.g., a crystalline absorber with passivated surfaces), TRPL decays would be single-exponential (linear when plotted on log-linear scale) [1]. This is not the case for CdS/CdTe absorbers. Therefore, two-exponential fitting is typically used

$$Intensity = A_1 \exp(-\frac{t}{\tau_1}) + A_2 \exp(-\frac{t}{\tau_2}) \quad (1)$$

where A_1/A_2 are amplitudes of components with lifetimes τ_1/τ_2. (Multi-exponential analysis is an approximation used under typical experimental conditions [1].) When decays have components with lifetimes <1ns, deconvolution of the instrumental response is used during fitting [5].

Fig. 3B shows τ_1 and τ_2 determined using two-exponential deconvolution for the data in Fig. 3A. For this sample, integration for 1s overestimates τ_1 and τ_2 values by about 15%. When integration time is increased between 5-120 s, τ_1 and τ_2 values are within the uncertainty range for the analysis. Therefore, a short integration time of 5 s is sufficient for characterization of a typical CdS/CdTe PV device. Data in Fig. 3 were collected with 1 MHz excitation. Because lifetimes for CdS/CdTe are short, higher repetition rate lasers could be used when measurement speed is critical. If, for example, one were to use a 20-MHz pulsed rate laser, a similar signal-to-noise level would be achieved in 20x shorter time (5 s / 20 = 250 s). Such measurement speed would potentially allow lifetime mapping in order to determine lateral lifetime variation in the polycrystalline semiconductor absorber film. Because in our approach excitation pulses are delivered and PL signals are collected using (the same) optical fiber, various fiber and/or sample scanning schemes can be implemented [4, 5].

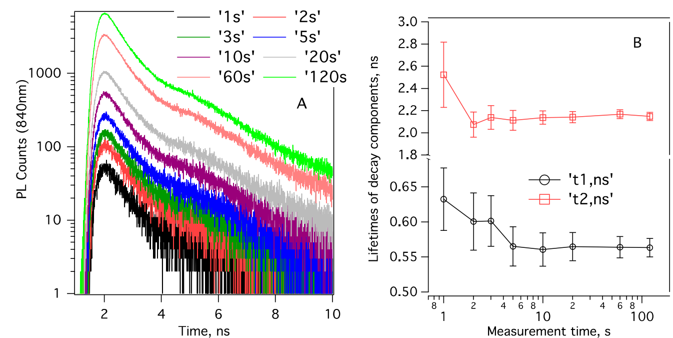

Fig. 3. A: TRPL decays for CdS/CdTe measured with integration for 1, 2, 3, 5, 10, 20, 60, and 120 seconds. B: Lifetimes determined after deconvolution with two-exponential fit function. Errors at 66% confidence level were determined using support plane analysis [6].

B. Absorber Characterization During CdS/CdTe PV Device Processing

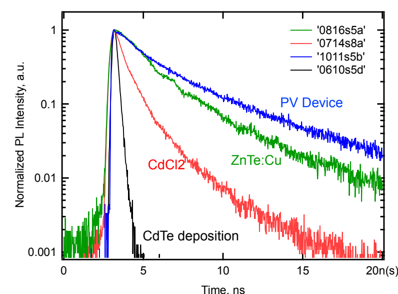

Fig. 4. Normalized TRPL decays for the same sample after CdTe deposition, $CdCl_2$ treatment, ZnTe:Cu application, and back contact formation. Excitation was through-glass (Fig. 1) using laser wavelength of 800 nm and 2 mW average power. Decays were measured at 840 nm.

Fig. 4 shows TRPL decays collected during CdS/CdTe PV device preparation at NREL [7]. Related data obtained using somewhat different excitation and sample preparation conditions were already reported [11]. First, after absorber deposition by CSS at 620°C, decay is very fast (87 ps). Decay becomes slower after $CdCl_2$ treatment at 400°C (τ_1 = 0.64 ns, τ_2 = 2.27 ns, $A_1/(A_1+A_2)$ = 0.86), after ZnTe:Cu sputtering (τ_1 = 1.55 ns, τ_2 = 4.23 ns, $A_1/(A_1+A_2)$ = 0.76), and finally after ITO/Ni/Al back-contact formation (τ_1 = 1.69 ns, τ_2 = 5.47 ns, $A_1/(A_1+A_2)$ = 0.64). Data shows that processing of the sample

has effects on the CdS/CdTe junction region, where the measurement is taken, and that all three parameters (τ_1, τ_2, and $A_1/(A_1+A_2)$) increase during processing. Increase in lifetimes indicates reduced recombination due to $CdCl_2$ and ZnTe:Cu processing steps. Amplitude change indicates carrier redistribution in the junction region as described below. In contrast to PL/TRPL, electrical measurements would not have been possible before PV device is fabricated. Thus, TRPL metrology could potentially detect changes in material properties before electrical characteristics of a PV device could be determined.

C. Carrier Dynamics at CdS/CdTe Interface

In order to describe carrier drift, diffusion, and recombination processes that give rise to two-exponential decays, we compare TRPL data measured for two CdS/CdTe PV devices. Device 2AA did not have intentional Cu doping, and device 2DA was fabricated using ZnTe with 2 wt.% Cu. SIMS depth profiles had shown that average Cu concentrations in the junction region were 3.4×10^{16} cm^{-3} and 8.5×10^{17} cm^{-3}, respectively [12]. Data for 2DA were shown in Fig. 1. The decays are clearly not-single exponential and differ depending on measurement wavelength. Two-exponential fitting with deconvolution of instrumental response provides excellent fit with all data. Therefore, a two-exponential global fitting was used. Global fitting implies that the same lifetimes are used for all decays, but amplitudes A_1 and A_2 depend on measurement wavelength. Time-resolved emission (TRES) spectra of amplitudes A_1 and A_2 (Eq. (1)) determined from such global analysis of 17 TRPL decays for devices 2AA and 2DA are shown in Fig. 5.

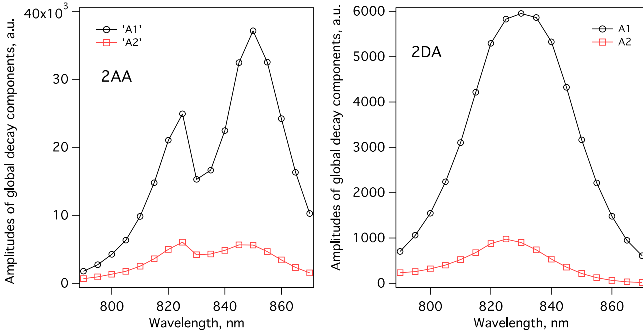

Fig. 5. TRES spectra for A_1 (τ_1) and A_2 (τ_2) decay components obtained by global analysis of TRPL data for CdS/CdTe devices 2AA and 2DA with different Cu doping. (For 2DA, TRPL data were shown in Fig. 1.) Excitation and measurement conditions were the same for both samples: λ_{ex} = 640 nm, average excitation power 2 mW, laser repetition rate 1 MHz, excitation beam diameter 0.17 mm, seventeen decays recorded every 5 nm at 790 – 870 nm.

We first consider TRES spectra for a CdS/CdTe PV device with no intentional Cu doping (2AA). Both faster (A_1; τ_1 = 0.36 ns) and slower (A_2; τ_2 = 1.69 ns) component spectra have maxima at 825 nm (1.50 eV) and the 850 nm (1.46 eV). The 825 nm peak is attributed to band-to-band CdTe emission and 850 nm peak to corresponding CdS_xTe_{1-x} emission. (PL spectra measured with excitation from the other side of the sample had only a 825 nm PL peak and confirmed its attribution to band-to-band recombination in CdTe.) Closer inspection shows that PL825 and PL850 amplitudes are different for A_1 and A_2 spectra. For A_2 PL850/PL825 $\approx$ 1 while for A_1 PL850/PL825 $\approx$ 1.5. Changes in TRES spectra indicate that PL corresponding to A_1 and A_2 components is emitted from different regions of the sample. For the faster decay component τ_1 (amplitude A_1), larger fraction of the emission arises in the CdS_xTe_{1-x} region, and the 850 nm peak is the strongest. This is consistent with the PV device structure in Fig. 1; 640 nm light is mostly absorbed in CdS_xTe_{1-x}, and emission from CdS_xTe_{1-x} is strongest for the initial part of the decay.

After photoexcitation with an ultrafast (0.3 ps) laser pulse, electron and hole distribution evolve over time. Such carrier redistribution is driven by the electric field of the pn junction (carrier drift) and also by diffusion due to the concentration gradient of photogenerated carriers. Over time, drift and diffusion lead to different carrier distribution. TRES spectrum for component A_2 provides evidence that charge redistribution did indeed take place. At the time range corresponding to the τ_2 decay component, emission from CdTe and CdS_xTe_{1-x} regions has approximately equal amplitude. Therefore, some fraction of photogenerated carriers have moved from CdS_xTe_{1-x} to CdTe; emission is stronger from CdTe but weaker from CdS_xTe_{1-x}. In summary, for τ_1, emission from CdS_xTe_{1-x} was the strongest; for τ_2, emissions from CdS_xTe_{1-x} and CdTe have equal intensity. Distinct time-resolved emission spectra from CdS_xTe_{1-x} and CdTe regions of the CdS/CdTe PV device, similar to the data shown here, have been reported in the literature [10].

A separate paper will report results of numerical simulations of TRPL decays that allow detailed analysis of drift and diffusion effects [8]. In agreement with the analysis of TRES spectra, it was determined that τ_1 represents charge separation in the electric field of the pn junction. Component τ_2 primarily arises due to recombination at the interface and in the "bulk" (Shockley–Read–Hall recombination). Therefore, accurate determination of τ_2 is important, as it provides the best experimental estimate of minority carrier lifetime – essential PV device characteristic. The limitation of τ_2 substitution for minority carrier lifetime is that the recombination extent at the interface vs. bulk cannot be determined.

Next, we consider TRES spectra for high-Cu device 2DA (Fig. 5B). Lifetimes τ_1 = 0.52 ns and τ_2 = 1.65 ns are similar to those for 2AA. Spectrum for A_2 has a peak at 825 nm – therefore, this emission is primarily from the CdTe region of the absorber. Spectrum for A_1 is only slightly red-shifted to 830 nm, but this spectrum is also is broader. This suggests that emission from both CdS_xTe_{1-x} and CdTe can be attributed to A_1 spectrum. Therefore dynamics reflected in TRES spectra is the same as for 2AA: component τ_1 reflects charge

separation, while component τ_2 reflects bulk and interface recombination.

Comparison of TRES spectra for CdS/CdTe PV devices 2AA and 2DA in Fig. 5 also suggests that Cu-doping has effects on carrier distribution in the junction region of the PV device. This effect will be analyzed in a future publication when Cu-doping in the junction region of the PV device will be systematically varied. Electrical characterization of this series of devices was reported [12]. The difference between electrical (JVT, CV, DLCP, AS) and optical (PL) characterization is that the former is more sensitive to carriers and defects in the bulk of the PV device [12], while the later is more sensitive to absorber properties at the CdS/CdTe interface.

Finally, we consider TRPL decays measured with 640 nm and 800 nm excitation. The goal of this measurement is to create different initial carrier distributions. The absorption coefficient at 640 nm is high, so 90% of excitation is absorbed in < 300 nm from the CdS_xTe_{1-x} interface. Near-bandgap 800 nm (1.55 eV) excitation is absorbed deeper. (Even longer excitation wavelengths could not be easily used in measurements, because scattered laser light would interfere with the weaker PL emission signal.) Fig. 6 shows several decays; Table 1 summarizes two-exponential fit parameters obtained with deconvolution of the instrumental response.

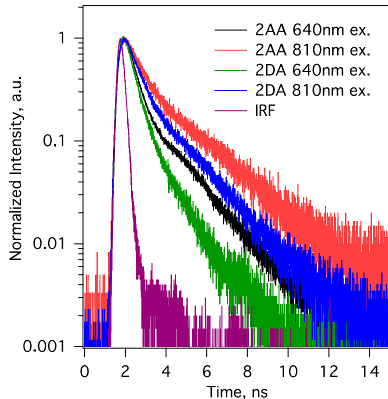

Fig. 6. Normalized TRPL decays for low-Cu (2AA) and high-Cu (2DA) samples measured with 640 nm and 800 nm excitation. Instrumental response function (IRF) is also shown.

Table 1. Two-exponential fit parameters for TRPL decays measured on low-Cu and high-Cu CdS/CdTe devices.

Excitation	Parameters	Low-Cu	High-Cu
640 nm	A_1, τ_1	85 %, 0.42 ns	87 %, 0.45 ns
	A_2, τ_2	15 %, 1.94 ns	13 %, 1.42 ns
800 nm	A_1, τ_1	66 %, 0.61 ns	74 %, 0.58 ns
	A_2, τ_2	34 %, 2.41 ns	26 %, 1.95 ns

When 800 nm excitation is used, amplitude A_1 decreases (for example, from 85% to 66% for low-Cu sample 2AA), while lifetimes τ_1 and τ_2 become somewhat longer. These data are in agreement with the simple two-region (CdS_xTe_{1-x} and CdTe) model described above. For example, as 800 nm radiation is absorbed deeper, initial (immediately after excitation) carrier distribution results in more carriers being in CdTe and somewhat away from the junction – thus amplitude of component A_1 is smaller with 800 nm excitation.

Larger τ_2 value with 800 nm excitation is in intuitive agreement with the interface recombination effects; when initial carrier distribution is further from the interface, surface recombination velocity has a smaller effect on recombination rate, thus τ_2 increases from 1.94 ns to 2.41 ns for 2AA and from 1.42 ns to 1.95 ns for 2DA. Interpreted this way, τ_2 value measured with near-bandgap excitation provides the best-experimental estimate for minority carrier lifetime; albeit "real" minority carrier lifetime is different, as surface recombination occurs at all excitation conditions. Numerical simulations of TRPL decays provide for accurate analysis of such effects [8].

Data presented in this section suggest that for single-excitation-wavelength TRPL measurements (for example, pulsed semiconductor lasers are less expensive and simpler excitation sources for TRPL but generate only at a narrow wavelength range) choosing near-bandgap excitation is somewhat preferable for CdS/CdTe PV device characterization. Using near-bandgap excitation somewhat reduces interface recombination and increases τ_2 amplitude – a desirable characteristic as, in principle, it allows shorter measurement time to obtain the same S/N for τ_2 determination. To unambiguously determine minority carrier lifetime, fabrication of an absorber with passivated surfaces would be necessary. Until such fabrication is implemented, computational modeling of TRPL data sometimes allows extraction of material and pn junction parameters [8]. In the absence of modeling, near-bandgap excitation and analysis of TRES spectra provides some insight into material and device characteristics.

IV. Conclusions

We described a novel optical scheme for a TRPL spectrometer. Measurements using optical fibers allow rapid and versatile characterization of thin film semiconductor absorbers. We have shown that TRPL data reflects CdS/CdTe absorber improvement during PV device manufacturing. It was shown that recombination is reduced due to well-known processes of annealing with $CdCl_2$ and due to Cu-doping. By analyzing time-resolved spectral changes and TRPL decays measured with different excitation wavelengths, we are able to analyze charge separation (τ_1) and recombination (τ_2). In conclusion, TRPL analysis is promising for online diagnostics/metrology and for studies of CdS/CdTe PV device physics.

ACKNOWLEDGMENTS

This work was supported by the U.S. Department of Energy under Contract No. DE-AC36-08-GO28308 with the National Renewable Energy Laboratory.

REFERENCES

[1] R. K. Ahrenkiel, Minority Carrier Lifetime in III-V Semiconductors, in *Semiconductors and Semimetals*, **39**, 1993, pp. 39-150

[2] W. K. Metzger D. Albin, D. Levi, P. Sheldon, X. Li, B. M. Keyes, B. R. K. Ahrenkiel, Time-Resolved Photoluminescence Studies of CdTe Solar Cells, *J. Appl. Phys.*, **94**, 2003, pp. 3549-55

[3] I. Repins, W. K. Metzger, C. L. Perkins, J. V. Li, M. A. Contreras, Correlation Between Measured Minority-Carrier Lifetime and Cu(In,Ga)Se_2 Device Performance, *Trans. on Electron Devices*, **57**, 2010, pp. 2957-63

[4] B. A. Flusberg, E. D. Cocker, W. Piyawattanametha, J. C. Jung, E. L. M. Cheung, M. J. Schnitzer, Fiber-optic fluorescence imaging, *Nature Methods*, **2**, 2005, pp. 941-50

[5] W. Becker, *Advanced Time-Correlated Single Photon Counting Techniques*, Springer, 2005

[6] *FluoFit Professional software*, PicoQuant GmbH

[7] J. N. Duenow, R. G. Dhere, J. V. Li, Jian M. R. Young, T. A. Gessert, Effects of Back-Contacting Methods and Temperature on CdTe/CdS Solar Cells, Proceedings *35th IEEE PVSC*, 2010, pp. 001001-5

[8] A. Kanevce, D. Kuciauskas, T. A. Gessert, D. H. Levi and David S. Albin, Impact of Interface Recombination on Time Resolved Photoluminescence Decays (TRPL) in CdTe solar cells (Numerical Simulation Analysis); these proceedings

[9] T. A. Gessert, W.K. Metzger, P. Dippo, S. E. Asher, R. G. Dhere, and M. R. Young, Dependence of Carrier Lifetime on Cu-contacting Temperature and ZnTe:Cu Thickness in CdS/CdTe Thin Film Solar Cells, *Thin Solid Films*, **517**, 2009, pp. 2370-73

[10] C. J. Bridge, P. Dawson, P. D. Buckle, and M. E. O zsan, Photoluminescence spectroscopy and decay time measurements of polycrystalline thin film CdTe/CdS solar cells, *J. Appl. Phys.* **88**, 2000, 6451-56

[11] W. K. Metzger, D. Albin, M. J. Romero, P. Dippo, and M. Young, $CdCl_2$ treatment, S diffusion, and recombination in polycrystalline CdTe, *J. Appl. Phys.* **99**, 2006, pp. 103703

[12] J. V. Li, J. N. Duenow, D. Kuciauskas, A. Kanevce, R. G. Dhere, M. R. Young, and D. H. Levi, Electrical Characterization of Cu Composition Effects in CdS/CdTe Thin-Film Solar Cells with a ZnTe:Cu Back Contact; these proceedings